**The University of Sydney**

School of Civil Engineering
Sydney NSW 2006
AUSTRALIA

http://www.civil.usyd.edu.au/

Centre for Advanced Structural Engineering

# Bifurcation of Locally Buckled Point Symmetric Columns – Analytical Developments

**Research Report No R866**

**Kim JR Rasmussen, MScEng, PhD**

**March 2006**

**ISSN 1833-2781**

The University of Sydney

**School of Civil Engineering**
**Centre for Advanced Structural Engineering**
**http://www.civil.usyd.edu.au/**

# Bifurcation of Locally Buckled Point Symmetric Columns – Analytical Developments

**Research Report No R866**

**Kim Rasmussen, MScEng, PhD**

**March 2006**

## Abstract:

The report derives the differential equations for the overall bifurcation of locally buckled point-symmetric columns. It is shown that flexural buckling about the minor and major principal axes are coupled in a locally buckled point-symmetric column whereas the buckling modes are uncoupled in a non-locally buckled column. The governing equations are solved for simply supported and fixed-ended columns and applied to Z-sections. Overall bifurcation curves are obtained for five Z-sections with increasingly slender flanges. It is shown that local buckling reduces the elastic torsional buckling load more so than the flexural buckling load for Z-sections, and that local buckling can cause a mode switch from the flexural to the torsional mode in Z-sections with very slender flanges.

## Keywords:

Z-sections, steel structures, local buckling, torsional buckling, flexural buckling, interaction buckling, finite strip analysis, bifurcation analysis.

## Copyright Notice

**School of Civil Engineering, Research Report R866**
**Bifurcation of Locally Buckled Point Symmetric Columns – Analytical Developments**

K.Rasmussen@civil.usyd.edu.au



Published by:
School of Civil Engineering
The University of Sydney
Sydney NSW 2006
AUSTRALIA

March 2006

This report and other Research Reports published by The School of Civil Engineering are available on the Internet:

http://www.civil.usyd.edu.au

# Table of Contents

# 1 Introduction

Thin-walled sections may suffer local buckling prior to overall collapse. In this case, it is important to know the influence of local buckling on the overall behaviour. Bifurcation analyses are particularly suited to study this influence and may be used to characterise the overall bifurcation behaviour for different types of cross-section.

The primary effect of local buckling is to reduce the member stiffnesses to overall flexure and torsion. Consequently, the overall bifurcation load can be calculated by using the stiffnesses of the locally buckled cross-section rather than the stiffness of the undistorted cross-section. This result has been used widely [1, 2] to determine the flexural buckling of locally buckled doubly symmetric columns. In this particular case, the buckling load can be obtained simply by replacing the flexural rigidity ($EI$) of the unbuckled section by the tangent, or effective, flexural rigidity of the locally buckled section in the Euler formula.

A general theory for calculating overall bifurcation loads (or buckling loads) of locally buckled members was presented in Ref [3]. The theory accounts for biaxial bending and torsion. It was applied to singly symmetric channel sections in compression by Young and Rasmussen [4, 5], and to doubly symmetric I-sections in compression and bending by Rasmussen and Hasham [6]. In the present paper, the theory is applied to point-symmetric sections in uniform compression. The buckling equations are first summarised and then used to calculate buckling curves for five different Z-sections with varying flange slenderness.

# 2 Buckling Equations

## 2.1 Model of the locally buckled member

The analytical model applies to cross-sections composed of thin plates. The component plates are assumed to buckle locally before overall buckling, such that plate deflections at junctions are negligible. This implies that the locally buckled state of the component plates can be described by the von Karman plate equations. Examples of the local buckling modes of point symmetric cross-sections in uniform compression are shown in Fig. 1.

By recognising that the effect of local buckling on the overall buckling behaviour is to reduce the stiffness of the member, a simple model can be devised by assuming that the locally buckled cross-section consists of an assembly of narrow strips, whose tangent stiffnesses ($E_t$) vary around the cross-section as a function of the extent of local buckling. The modeling allows the effect of local buckling, which cause a *geometrical* loss of stiffness to be considered as a *material* effect in the overall bifurcation analysis, in so far that the effect is to change the initial stiffness ($E$). Consequently, it allows the theory for the buckling of thin-walled members, with an *undistorted* cross-section, to be used by changing only the stress-strain relations [3]. Furthermore, the effect of yielding can be taken into account when calculating the stiffness of the various points in the cross-section.

The governing equations derived in [3] are expressed in terms of the generalised displacements ($u$, $v$, $w$, $\phi$), which are assumed to refer to the shear centre of the undistorted cross-section. The formulation uses a set of tangent rigidities, defined as

$$(EA)_t = \int_A E_t^{w'}\, dA \tag{1}$$

$$(ES_x)_t = \int_A E_t^{w'} y\, dA = \int_A E_t^{v''} y\, dA \tag{2}$$

$$(ES_y)_t = \int_A E_t^{w'} x\, dA = \int_A E_t^{u''} x\, dA \tag{3}$$

$$(ES_\omega)_t = \int_A E_t^{w'} \omega\, dA = \int_A E_t^{\phi''} \omega\, dA \tag{4}$$

$$(EI_x)_t = \int_A E_t^{v''} y^2\, dA \tag{5}$$

$$(EI_y)_t = \int_A E_t^{u''} x^2\, dA \tag{6}$$

$$(EI_\omega)_t = \int_A E_t^{\phi''} \omega^2\, dA \tag{7}$$

$$(EI_{xy})_t = \int_A E_t^{v''} xy\, dA = \int_A E_t^{u''} xy\, dA \tag{8}$$

$$(EI_{x\omega})_t = \int_A E_t^{\phi''} y\omega\, dA = \int_A E_t^{v''} y\omega\, dA \tag{9}$$

$$(EI_{y\omega})_t = \int_A E_t^{\phi''} x\omega\, dA = \int_A E_t^{u''} x\omega\, dA \tag{10}$$

$$(GJ)_t = \int_A G_t\, 4n^2\, dA \tag{11}$$

where ($x$,$y$) are principal coordinates, and the tangent rigidity against shear ($G_t$) may be assumed to be equal to the full shear modulus $G$ [7]. The tangent moduli, $E_t^{w'}, E_t^{u''}, E_t^{v''}, E_t^{\phi''}$, are the stiffnesses against axial straining ($w'$), bending in the ($x$,$z$)-plane ($u''$), bending in the ($y$,$z$)-plane ($v''$) and twisting ($\phi''$) respectively, such that the incremental longitudinal stress is given by,

$$\dot{\sigma} = E_t^{w'}\dot{w}' + E_t^{u''}x(-\dot{u}'') + E_t^{v''}y(-\dot{v}'') + E_t^{\phi''}\omega(-\dot{\phi}''). \tag{12}$$

## 2.2 General bifurcation equation

As derived in [3], the general variational equation of incremental equilibrium of the fundamental state is given by,

$$\int_L \begin{Bmatrix} \dot{w}_0' \\ -\dot{u}_0'' \\ -\dot{v}_0'' \\ -\dot{\phi}_0'' \\ -\dot{\phi}_0' \end{Bmatrix}^T \begin{bmatrix} (EA)_t & (ES_y)_t & (ES_x)_t & (ES_\omega)_t & 0 \\ (ES_y)_t & (EI_y)_t & (EI_{xy})_t & (EI_{y\omega})_t & 0 \\ (ES_x)_t & (EI_{xy})_t & (EI_x)_t & (EI_{x\omega})_t & 0 \\ (ES_\omega)_t & (EI_{y\omega})_t & (EI_{x\omega})_t & (EI_\omega)_t & 0 \\ 0 & 0 & 0 & 0 & (GJ)_t \end{bmatrix} \begin{Bmatrix} \delta w_0' \\ -\delta u'' \\ -\delta v'' \\ -\delta\phi'' \\ -\delta\phi' \end{Bmatrix} dz$$
$$- \dot{\lambda}\left[\overline{N}\,\delta w + \overline{M}_y\,\delta u' + \overline{M}_x(-\delta v') + \overline{B}(-\delta\phi')\right]_{0,L} = 0 \tag{13}$$

where $\delta(\ )$ denotes a virtual quantity, $\dot{w}_0, \dot{u}_0, \dot{v}_0, \dot{\phi}_0$ are increments of fundamental state displacements, $\overline{N}, \overline{M}_x, \overline{M}_y, \overline{B}$ are applied reference stress resultants, defined by

$$\overline{N} = \int_A q_z \, dA \tag{14}$$

$$\overline{M}_y = -\int_A q_z x \, dA \tag{15}$$

$$\overline{M}_x = \int_A q_z y \, dA \tag{16}$$

$$\overline{B} = \int_A q_z \omega \, dA \tag{17}$$

in which $q_z$ is a longitudinal reference stress applied at the ends, and $\dot{\lambda}$ is the incremental load factor, such that the total applied stress resultants are $\lambda\overline{N}, \lambda\overline{M}_x, \lambda\overline{M}_y, \lambda\overline{B}$.

The incremental internal stress resultants of the fundamental state are defined as

$$\dot{N}_0 = \int_A \dot{\sigma}_0 \, dA \tag{18}$$

$$\dot{M}_{x_0} = \int_A \dot{\sigma}_0 y \, dA \tag{19}$$

$$\dot{M}_{y_0} = -\int_A \dot{\sigma}_0 x \, dA \tag{20}$$

$$\dot{B}_0 = \int_A \dot{\sigma}_0 \omega \, dA \tag{21}$$

where $\dot{\sigma}_0$ is the incremental longitudinal fundamental state stress.

The general variational equation of bifurcation is given by [3],

$$\int_L \begin{Bmatrix} w_b' \\ -u_b'' \\ -v_b'' \\ -\phi_b'' \\ -\phi_b' \end{Bmatrix}^T \begin{bmatrix} (EA)_t & (ES_y)_t & (ES_x)_t & (ES_\omega)_t & 0 \\ (ES_y)_t & (EI_y)_t & (EI_{xy})_t & (EI_{y\omega})_t & 0 \\ (ES_x)_t & (EI_{xy})_t & (EI_x)_t & (EI_{x\omega})_t & 0 \\ (ES_\omega)_t & (EI_{y\omega})_t & (EI_{x\omega})_t & (EI_\omega)_t & 0 \\ 0 & 0 & 0 & 0 & (GJ)_t \end{bmatrix} \begin{Bmatrix} \delta w' \\ -\delta u'' \\ -\delta v'' \\ -\delta\phi'' \\ -\delta\phi' \end{Bmatrix} dz$$

$$+ \int_L \begin{Bmatrix} u_b' \\ u_b'' \\ v_b' \\ v_b'' \\ \phi_b' \\ \phi_b'' \end{Bmatrix}^T \begin{bmatrix} N_0 & 0 & 0 & 0 & 0 & y_S N_0 \\ 0 & 0 & 0 & 0 & M_{x_0} & 0 \\ 0 & 0 & N_0 & 0 & 0 & -x_S N_0 \\ 0 & 0 & 0 & 0 & M_{y_0} & 0 \\ 0 & M_{x_0} & 0 & M_{y_0} & 0 & 0 \\ y_S N_0 & 0 & -x_S N_0 & 0 & 0 & (x_S^2 + y_S^2)N_0 + W_0 \\ & & & & & + 2x_S M_{y_0} - 2y_S M_{x_0} \end{bmatrix} \begin{Bmatrix} \delta u' \\ \delta u'' \\ \delta v' \\ \delta v'' \\ \delta\phi' \\ \delta\phi'' \end{Bmatrix} dz$$

$$- \left[ \lambda_c \overline{M}_y (\phi_b \, \delta v + v_b' \, \delta\phi) + \lambda_c \overline{M}_x (\phi_b \, \delta u' + u_b' \, \delta\phi) \right]_{0,L} = 0 \tag{22}$$

where $w_b, u_b, v_b, \phi_b$ are the buckling displacements, $N_0, M_{x_0}, M_{y_0}$ are the fundamental state stress resultants, ($x_S$, $y_S$) are the shear centre coordinates, $\lambda_c$ is the critical load factor, and $W_0$ is the Wagner stress resultant defined as,

$$W_0 = -\lambda \overline{W} \tag{23}$$

where

$$\overline{W} = -\int_A \sigma_0 (x^2 + y^2)\, dA / \lambda. \tag{24}$$

## 2.3 Point symmetric cross-sections in compression

### 2.3.1 Fundamental state

The ($x$,$y$)-axes are assumed to be principal, as shown in Fig. 1, and the sectorial coordinate ($\omega$) is assumed to be normalized and referring to the shear centre. It then follows from the point symmetry that $\omega$ is an even function of $x$ and $y$,

$$\omega(x, y) = \omega(-x,-y). \tag{25}$$

Since the local buckling deformations of a point symmetric cross-section are symmetric in magnitude with respect to the point of symmetry, the tangential stiffnesses ($E_t^{w'}, E_t^{u''}, E_t^{v''}, E_t^{\phi''}$) are even functions of $x$ and $y$,

$$E_t(x, y) = E_t(-x,-y). \tag{26}$$

Using eqns (25, 26), it follows from eqns (2, 3, 9, 10) that

$$(ES_x)_t = (ES_y)_t = (EI_{x\omega})_t = (EI_{y\omega})_t = 0 \tag{27}$$

so that the incremental equilibrium equation (13) becomes,

$$\int_L \begin{Bmatrix} \dot{w}_0' \\ -\dot{u}_0'' \\ -\dot{v}_0'' \\ -\dot{\phi}_0'' \\ -\dot{\phi}_0' \end{Bmatrix}^T \begin{bmatrix} (EA)_t & 0 & 0 & (ES_\omega)_t & 0 \\ 0 & (EI_y)_t & (EI_{xy})_t & 0 & 0 \\ 0 & (EI_{xy})_t & (EI_x)_t & 0 & 0 \\ (ES_\omega)_t & 0 & 0 & (EI_\omega)_t & 0 \\ 0 & 0 & 0 & 0 & (GJ)_t \end{bmatrix} \begin{Bmatrix} \delta w_0' \\ -\delta u'' \\ -\delta v'' \\ -\delta \phi'' \\ -\delta \phi' \end{Bmatrix} dz$$
$$- \lambda \left[ \overline{N}\, \delta w + \overline{M}_y\, \delta u' + \overline{M}_x (-\delta v') + \overline{B} (-\delta \phi') \right]_{0,L} = 0. \tag{28}$$

By expanding and integrating this equation by parts, the following differential equations and boundary conditions are obtained,

*Differential equations:*

$$\left( (EA)_t\, \dot{w}_0' \right)' - \left( (ES_\omega)_t\, \dot{\phi}_0'' \right)' = 0 \tag{29}$$

$$-\left((ES_\omega)_t\,\dot{w}_0'\right)'' + \left((EI_\omega)_t\,\dot{\phi}_0''\right)'' - \left((GJ)_t\,\dot{\phi}_0'\right)' = 0 \tag{30}$$

$$\left((EI_y)_t\,\dot{u}_0''\right)'' + \left((EI_{xy})_t\,\dot{v}_0''\right)'' = 0 \tag{31}$$

$$\left((EI_{xy})_t\,\dot{u}_0''\right)'' + \left((EI_x)_t\,\dot{v}_0''\right)'' = 0 \tag{32}$$

*Boundary conditions:*
The boundary conditions are listed in Table 1 as derived from the variations equation (28). In the table, the upper and lower stacked signs ($\pm$ or $\mp$) refer to $z$=0 and $z$=$L$, respectively.

| Geometric quantity restrained | or Geometric quantity unrestrained | Eqn |
|---|---|---|
| $\dot{w}_0 = 0$ | $\left((EA)_t\,\dot{w}_0'\right) - \left((ES_\omega)_t\,\dot{\phi}_0''\right) \pm \dot{\lambda}\overline{N} = 0$ | (33a,b) |
| $\dot{u}_0 = 0$ | $\left((EI_y)_t\,\dot{u}_0''\right)' + \left((EI_{xy})_t\,\dot{v}_0''\right)' = 0$ | (34a,b) |
| $\dot{u}_0' = 0$ | $\left((EI_y)_t\,\dot{u}_0''\right) + \left((EI_{xy})_t\,\dot{v}_0''\right) \pm \dot{\lambda}\overline{M}_y = 0$ | (35a,b) |
| $\dot{v}_0 = 0$ | $\left((EI_{xy})_t\,\dot{u}_0''\right)' + \left((EI_x)_t\,\dot{v}_0''\right)' = 0$ | (36a,b) |
| $\dot{v}_0' = 0$ | $\left((EI_{xy})_t\,\dot{u}_0''\right) + \left((EI_x)_t\,\dot{v}_0''\right) \mp \dot{\lambda}\overline{M}_x = 0$ | (37a,b) |
| $\dot{\phi}_0 = 0$ | $\left((ES_\omega)_t\,\dot{w}_0'\right)' - \left((EI_\omega)_t\,\dot{\phi}_0''\right)' + (GJ)_t\,\dot{\phi}_0' = 0$ | (38a,b) |
| $\dot{\phi}_0' = 0$ | $-\left((ES_\omega)_t\,\dot{w}_0'\right) + \left((EI_\omega)_t\,\dot{\phi}_0''\right) \mp \dot{\lambda}\overline{B} = 0$ | (39a,b) |

$\pm, \mp$ upper sign refers to $z$=0, lower to $z$=$L$

Table 1: Boundary conditions for the fundamental state. Columns with point symmetric thin-walled cross-sections.

It follows from eqns (29-39) that $w_0$ and $\phi_0$ are coupled and that $u_0$ and $v_0$ are coupled in the fundamental state, while there is no coupling between ($w_0$, $\phi_0$) and ($u_0$, $v_0$).

*Simply supported and fixed ended columns*
The geometric boundary conditions and applied actions for simply supported and fixed-ended columns are shown in Figs 2 and 3 respectively. Combined with Table 1, they provide the boundary conditions for the fundamental state. Note that warping is assumed to be restrained ( $\phi_0' = 0$ ) at the ends for both the simply supported and fixed-ended cases.

As will be shown in the following, the tangent rigidities can be assumed to be constant along the length for any given axial load in the fundamental state. By differentiating and combining eqns (29-32) under this assumption, the following equations are obtained,

$$\left((EI_\omega)_t - \frac{(ES_\omega)_t^2}{(EA)_t}\right)\dot{\phi}_0'''' - (GJ)_t\,\dot{\phi}_0'' = 0 \tag{40}$$

$$\left((EI_x)_t - \frac{(EI_{xy})_t^2}{(EI_y)_t}\right)\dot{v}_0'''' = 0 \tag{41}$$

$$\dot{w}_0'' = \frac{(ES_\omega)_t}{(EA)_t}\,\dot{\phi}_0''' \tag{42}$$

$$\dot{u}_0'''' = -\frac{(EI_{xy})_t}{(EI_y)_t}\dot{v}_0'''' \tag{43}$$

These equations are readily solved for $\dot{w}_0, \dot{u}_0, \dot{v}_0, \dot{\phi}_0$ and combined with eqns (33a&b,34a, 35b,36a,37b,38a,39a) for simply supported columns and eqns (33a&b,34a,35a,36a,37a,38a, 39a) for fixed-ended columns. In either case, the equations lead to

$$\dot{w}_0 = -\frac{\dot{\lambda}\overline{N}}{(EA)_t} z \tag{44}$$

$$\dot{u}_0 = \dot{v}_0 = \dot{\phi}_0 = 0. \tag{45}$$

This result shows that the axial straining is uniform along the length and hence confirms the assumption that the tangent rigidities are constant.

Using eqns (1-12), (18-20), (27), the incremental stress resultants are obtained as,

$$\dot{N}_0 = -\dot{\lambda}\overline{N} \tag{46}$$

$$\dot{M}_{x_0} = 0 \tag{47}$$

$$\dot{M}_{y_0} = 0 \tag{48}$$

$$\dot{B}_0 = -\frac{(ES_\omega)_t}{(EA)_t}\dot{\lambda}\overline{N}. \tag{49}$$

It follows that the stress resultants for simply supported and fixed-ended columns are:

$$N_0 = -\lambda\overline{N} \tag{50}$$

$$M_{x_0} = 0 \tag{51}$$

$$M_{y_0} = 0 \tag{52}$$

$$B_0 = -\int \frac{(ES_\omega)_t}{(EA)_t}\overline{N}\, d\lambda. \tag{53}$$

This result demonstrates that a bimoment develops in the fundamental state of an axially loaded locally buckled point symmetric column.

### 2.3.2 Bifurcated state

By using eqn. (27) and the stress resultants given by eqns (50-53), the bifurcation equation (22) for axially loaded simply supported and fixed-ended point symmetric columns becomes,

$$\int_L \begin{Bmatrix} w_b' \\ -u_b'' \\ -v_b'' \\ -\phi_b'' \\ -\phi_b' \end{Bmatrix}^T \begin{bmatrix} (EA)_t & 0 & 0 & (ES_\omega)_t & 0 \\ 0 & (EI_y)_t & (EI_{xy})_t & 0 & 0 \\ 0 & (EI_{xy})_t & (EI_x)_t & 0 & 0 \\ (ES_\omega)_t & 0 & 0 & (EI_\omega)_t & 0 \\ 0 & 0 & 0 & 0 & (GJ)_t \end{bmatrix} \begin{Bmatrix} \delta w' \\ -\delta u'' \\ -\delta v'' \\ -\delta\phi'' \\ -\delta\phi' \end{Bmatrix} dz$$

$$+\lambda_c \int_L \begin{Bmatrix} u_b' \\ u_b'' \\ v_b' \\ v_b'' \\ \phi_b' \\ \phi_b'' \end{Bmatrix}^T \begin{bmatrix} -\overline{N} & 0 & 0 & 0 & 0 & 0 \\ 0 & 0 & 0 & 0 & 0 & 0 \\ 0 & 0 & -\overline{N} & 0 & 0 & 0 \\ 0 & 0 & 0 & 0 & 0 & 0 \\ 0 & 0 & 0 & 0 & 0 & 0 \\ 0 & 0 & 0 & 0 & 0 & -\overline{W} \end{bmatrix} \begin{Bmatrix} \delta u' \\ \delta u'' \\ \delta v' \\ \delta v'' \\ \delta\phi' \\ \delta\phi'' \end{Bmatrix} dz = 0. \tag{54}$$

By expanding and integrating by parts, the following differential equations and boundary conditions are obtained,

*Differential equations:*

$$\left((EA)_t \dot{w}_b'\right)' - \left((ES_\omega)_t \dot{\phi}_b''\right)' = 0 \tag{55}$$

$$-\left((ES_\omega)_t \dot{w}_b'\right)'' + \left((EI_\omega)_t \dot{\phi}_b''\right)'' - \left((GJ)_t \phi_b'\right)' + \left(\lambda_c \overline{W} \phi_b'\right)' = 0 \tag{56}$$

$$\left((EI_y)_t \dot{u}_b''\right)'' + \left((EI_{xy})_t \dot{v}_b''\right)'' + \left(\lambda_c \overline{N} u_b'\right)' = 0 \tag{57}$$

$$\left((EI_{xy})_t \dot{u}_b''\right)'' + \left((EI_x)_t \dot{v}_b''\right)'' + \left(\lambda_c \overline{N} v_b'\right) = 0 \tag{58}$$

*Boundary conditions:*
The boundary conditions are listed in Table 2 as derived from the variation equation (54).

| Geometric quantity restrained | or Geometric quantity unrestrained | Eqn |
|---|---|---|
| $w_b = 0$ | $\left((EA)_t w_b'\right) - \left((ES_\omega)_t \phi_b''\right) = 0$ | (59a,b) |
| $u_b = 0$ | $\left((EI_y)_t u_b''\right)' + \left((EI_{xy})_t v_b''\right)' + \lambda_c \overline{N} u_b' = 0$ | (60a,b) |
| $u_b' = 0$ | $\left((EI_y)_t u_b''\right) + \left((EI_{xy})_t v_b''\right) = 0$ | (61a,b) |
| $v_b = 0$ | $\left((EI_{xy})_t u_b''\right)' + \left((EI_x)_t v_b''\right)' + \lambda_c \overline{N} v_b' = 0$ | (62a,b) |
| $v_b' = 0$ | $\left((EI_{xy})_t u_b''\right) + \left((EI_x)_t v_b''\right)_x = 0$ | (63a,b) |
| $\phi_b = 0$ | $\left((ES_\omega)_t w_b'\right)' - \left((EI_\omega)_t \phi_b''\right)' + (GJ)_t \phi_b' - \lambda_c \overline{W} \phi_b' = 0$ | (64a,b) |
| $\phi_b' = 0$ | $-\left((ES_\omega)_t w_b'\right) + \left((EI_\omega)_t \phi_b''\right) = 0$ | (65a,b) |

$\pm, \mp$ upper sign refers to $z$=0, lower to $z$=$L$

Table 2: Boundary conditions for the bifurcated state. Simply supported and fixed-ended columns with point symmetric thin-walled cross-section.

It follows from eqns (55-65) that the flexural buckling displacements ($u_b$, $v_b$) are coupled when the section is locally buckled. The coupling arises because of the term $(EI_{xy})_t$ which

increases gradually as local buckling develops. The term is zero for non-locally buckled sections and accordingly, the minor and major axis flexural buckling modes are uncoupled for non-locally buckled columns. From a physical viewpoint, the coupling between $u_b$ and $v_b$ in a locally buckled section means that overall flexural buckling occurs about an axis which is rotated from the minor principal axis. The axis of flexure changes because the stiffness of the section changes non-uniformly within the cross-section. Torsional buckling involves ($w_b$, $\varphi_b$) and is uncoupled from flexural buckling.

The differential equations (55-58) and boundary conditions (59-65) for simply supported and fixed-ended columns can be satisfied by the following displacement fields:
*Simply supported columns*:

$$\frac{u_b}{C_u} = \frac{v_b}{C_v} = \sin\left(\frac{\pi z}{L}\right) \tag{66}$$

$$\frac{w_b}{C_w} = \sin\left(\frac{2\pi z}{L}\right) \tag{67}$$

$$\frac{\phi_b}{C_\phi} = \left(1 - \cos\left(\frac{2\pi z}{L}\right)\right). \tag{68}$$

*Fixed-ended columns*:

$$\frac{u_b}{C_u} = \frac{v_b}{C_v} = \frac{\phi_b}{C_\phi} = \left(1 - \cos\left(\frac{2\pi z}{L}\right)\right) \tag{69}$$

$$\frac{w_b}{C_w} = \sin\left(\frac{2\pi z}{L}\right). \tag{70}$$

By substituting these equations into the differential equations (55-58) and requiring non-trivial solutions, the following determinant equation is obtained,

$$\begin{vmatrix} (EA)_t & -\frac{2\pi}{L}(ES_\omega)_t & 0 & 0 \\ -\frac{2\pi}{L}(ES_\omega)_t & \left(\frac{2\pi}{L}\right)^2 (EI_\omega)_t + (GJ)_t - \lambda_c \overline{W} & 0 & 0 \\ 0 & 0 & \left(\frac{k\pi}{L}\right)^2 (EI_y)_t - \lambda_c \overline{N} & \left(\frac{k\pi}{L}\right)^2 (EI_{xy})_t \\ 0 & 0 & \left(\frac{k\pi}{L}\right)^2 (EI_{xy})_t & \left(\frac{k\pi}{L}\right)^2 (EI_x)_t - \lambda_c \overline{N} \end{vmatrix} = 0 \tag{71}$$

where $k$=1 for simply supported columns and $k$=2 for fixed-ended columns. The first two rows of eqn. (71) pertain to the longitudinal displacement ($w_b$) and twist rotation ($\phi_b$), while the latter two rows pertain to the flexural displacements ($u_b$,$v_b$). The critical load factors for flexural buckling ( $\lambda_{c_{uv}}$ ) and torsional buckling ( $\lambda_{c_\phi}$ ) are readily obtained from eqn. (71),

$$\lambda_{c_{uv}} = \frac{1}{2\overline{N}}\left(\frac{k\pi}{L}\right)^2\left[\underline{\left((EI_x)_t + (EI_y)_t\right)} \pm \left\{\underline{\left((EI_x)_t + (EI_y)_t\right)^2} - 4\left(\underline{\underline{(EI_x)_t(EI_y)_t - (EI_{xy})_t^2}}\right)\right\}^{\frac{1}{2}}\right] \tag{72}$$

$$\lambda_{c_\phi} = \frac{1}{\overline{W}}\left[\left(\frac{2\pi}{L}\right)^2 (EI_\omega)_t + (GJ)_t - \left(\frac{2\pi}{L}\right)^2 \frac{(ES_\omega)_t^2}{(EA)_t}\right] \tag{73}$$

The critical loads are to be obtained as,

$$N_{c_{uv}} = \lambda_{c_{uv}}\overline{N} \tag{74}$$

$$N_{c_\phi} = \lambda_{c_\phi}\overline{N} = \frac{\overline{N}}{\overline{W}}\left[\left(\frac{2\pi}{L}\right)^2 (EI_\omega)_t + (GJ)_t - \left(\frac{2\pi}{L}\right)^2 \frac{(ES_\omega)_t^2}{(EA)_t}\right] \tag{75}$$

where $\overline{W}$ is given by eqn. (24).

# 3 Tangent rigidities

## 3.1 Computational procedure

As discussed in detail in [2-4], the tangent rigidities defined by eqns (1-10) can be obtained from a non-linear post-local buckling analysis by subjecting a single local buckle to increasing levels of axial compression and at each compression level, superimposing onto the locally buckled state a small increment of generalised strain ($\Delta w', -\Delta u'', -\Delta v'', -\Delta\phi''$). The numerical process requires the internal stress resultants ($\Delta N, \Delta M_x, \Delta M_y, \Delta B$) be calculated for each superimposed increment of generalised strain. The tangent rigidities are then the ratios of internal stress resultant to generalised strain. For instance,

$$(EA)_t = \frac{\partial N}{\partial w'} \cong \frac{\Delta N}{\Delta w'} \tag{76}$$

$$(ES_\omega)_t = \frac{\partial B}{\partial w'} \cong \frac{\Delta B}{\Delta w'} \tag{77}$$

$$(EI_x)_t = \frac{\partial M_x}{-\partial v''} \cong \frac{\Delta M_x}{-\Delta v''} \tag{78}$$

$$(EI_{xy})_t = \frac{\partial M_y}{-\partial v''} \cong \frac{\Delta M_y}{-\Delta v''} \quad \text{or} \quad (EI_{xy})_t = \frac{\partial M_x}{-\partial u''} \cong \frac{\Delta M_x}{-\Delta u''}, \quad \text{etc.} \tag{79}$$

The generalised strains ($\Delta w', -\Delta u'', -\Delta v'', -\Delta\phi''$) are superimposed by applying small uniform displacements, rotational displacements or warping displacements onto the current locally buckled state. For instance, the curvature ($-\Delta u''$) is introduced by applying equal and opposite rotations ($\Delta u'$) and the two ends of a local buckle of length *l*, so that,

$$-\Delta u'' = -\frac{2\Delta u'}{l} \tag{80}$$

The post-local buckling analysis may typically be carried out using a non-linear elastic finite strip analysis [8] or an inelastic nonlinear finite strip analysis [9].

## 3.2 Invariants

The principal axes of point symmetric sections, such as plain or lipped Z-sections, are usually rotated relative to the parallel axes defined by the component plates. In this case, it becomes cumbersome to calculate the displacements arising from the superimposed rotations $(\Delta u', \Delta v')$ about the principal axes,

$$w^{u''} = \Delta u' x \tag{80}$$
$$w^{v''} = -\Delta v' y \tag{81}$$

However, as will be show in the following, in calculating the flexural buckling load ($N_{c_{uv}}$), the underlined terms $\left((EI_x)_t + (EI_y)_t\right)$ and $\left((EI_x)_t (EI_y)_t - (EI_{xy})_t^2\right)$ of eqn. (72) are invariant to the choice of coordinate system. Consequently, the tangent moduli terms ($(EI_x)_t$, $(EI_{xy})_t$, etc) can be calculated with reference to a convenient orthogonal $(\bar{x}, \bar{y})$-system aligned with the component plates of the cross-section, such as the web and flanges of a Z-section.

The existence of invariants can be proved on the basis of the reciprocal theorem. We consider first the displacements arising from rotations about the principal (*x*,*y*) axes, as given by eqns (80,81), and the associated longitudinal stresses,

$$\sigma^{u''} = E_t^{u''} \frac{2\Delta u'}{l} x \tag{82}$$
$$\sigma^{v''} = -E_t^{v''} \frac{2\Delta v'}{l} y \tag{83}$$

as shown in Fig. 4c. The stresses $(\sigma^{u''}, \sigma^{v''})$ are those which develop in addition to the post-local buckling stresses present in the fundamental state, which are shown in Fig. 4a.

The corresponding displacements and stresses for superimposed rotations $(\Delta\bar{u}', \Delta\bar{v}')$ about the orthogonal axes are:

$$w^{\bar{u}''} = \Delta\bar{u}' \bar{x} \tag{84}$$
$$w^{\bar{v}''} = -\Delta\bar{v}' \bar{y} \tag{85}$$
$$\sigma^{\bar{u}''} = E_t^{\bar{u}''} \frac{2\Delta\bar{u}'}{l} \bar{x} \tag{86}$$
$$\sigma^{\bar{v}''} = -E_t^{\bar{v}''} \frac{2\Delta\bar{v}'}{l} \bar{y} \tag{87}$$

as shown in Fig. 4b. The following equalities follow from the reciprocal theorem,

$$\int_A \sigma^{\bar{u}''} w^{u''} \, dA = \int_A \sigma^{u''} w^{\bar{u}''} \, dA \tag{88}$$
$$\int_A \sigma^{\bar{v}''} w^{v''} \, dA = \int_A \sigma^{v''} w^{\bar{v}''} \, dA \tag{89}$$
$$\int_A \sigma^{\bar{u}''} w^{v''} \, dA = \int_A \sigma^{v''} w^{\bar{u}''} \, dA \tag{90}$$

By substituting eqns (80-87) into this equation and using the transformation,

$$\bar{x} = x\cos\alpha + y\sin\alpha \tag{92}$$
$$\bar{y} = -x\sin\alpha + y\cos\alpha \tag{93}$$

where α is the rotation between the two coordinate systems (Fig. 4c), the following equations result,

$$\cos\alpha(EI_{\bar{x}})_t - \sin\alpha(EI_{\overline{xy}})_t = \cos\alpha(EI_x)_t + \sin\alpha(EI_{xy})_t \quad (94)$$

$$\cos\alpha(EI_{\bar{y}})_t + \sin\alpha(EI_{\overline{xy}})_t = \cos\alpha(EI_y)_t - \sin\alpha(EI_{xy})_t \quad (95)$$

$$-\sin\alpha(EI_{\bar{y}})_t + \cos\alpha(EI_{\overline{xy}})_t = -\sin\alpha(EI_x)_t + \cos\alpha(EI_{xy})_t \quad (96)$$

where $(EI_{\bar{x}})_t, (EI_{\bar{y}})_t, (EI_{\overline{xy}})_t$ are defined as,

$$(EI_{\bar{x}})_t = \int_A E_t^{\bar{v}''}\bar{y}^2\,dA \quad (97)$$

$$(EI_{\bar{y}})_t = \int_A E_t^{\bar{u}''}\bar{x}^2\,dA \quad (98)$$

$$(EI_{\overline{xy}})_t = \int_A E_t^{\bar{u}''}\overline{xy}\,dA = \int_A E_t^{\bar{v}''}\overline{xy}\,dA. \quad (99)$$

Solving eqns (94-96) for the tangent rigidities $((EI_x)_t, (EI_y)_t, (EI_{xy})_t)$, the following results can be shown:

$$(EI_x)_t + (EI_y)_t = (EI_{\bar{x}})_t + (EI_{\bar{y}})_t \quad (100)$$

$$(EI_x)_t(EI_y)_t - (EI_{xy})_t^2 = (EI_{\bar{x}})_t(EI_{\bar{y}})_t - (EI_{\overline{xy}})_t^2 \quad (101)$$

which prove that the terms of eqn. (72) are invariant to the choice of coordinate system.

# 4 Buckling Curves for Fixed-ended Z-section Columns

Five cross-sections were selected for studying the bifurcation behaviour of thin-walled Z-section columns. All sections had the same thickness (1.5 mm) and web depth (100 mm). Different flange widths were used to produce ratios ($\sigma_{l,f}/\sigma_{l,w}$) of local buckling stress of the flanges to local buckling stress of the web of 0.25, 0.5, 1, 2 and 4. These ratios were calculated using local buckling coefficients ($k$) of 0.425 and 4 for the flanges and web respectively. The cross-sections are detailed in Fig. 5 together with the local buckling stress ($\sigma_l$) and half-wavelength ($l$) for each cross-section, as determined from a rational elastic buckling analysis treating the section as a plate assemblage [9]. The figure also shows the orientation of the principal ($x$,$y$)-axes for each cross-section.

Local buckling of the 16.3- and 23.0-sections was triggered by instability of the web and so the stress redistribution developing in the post-local buckling range occurred mainly in the web. For the 32.6-section, the web and flanges were affected by local buckling to comparable degrees, whereas for the 46.1- and 65.2-sections, local buckling and the stress redistribution developing in the post-local buckling range occurred mainly in the flanges.

The overall buckling loads were obtained according to classical theory (assuming elastic behaviour and no cross-sectional distortion), elastic theory (allowing cross-sectional distortion, ie local buckling) and inelastic theory (allowing cross-sectional distortion and yielding). In the inelastic analyses, the material was assumed to be linear-perfectly-plastic with yield stress values of 1, 2 and 3 times the elastic local buckling stress. For instance, for

the 16.3-section, the local buckling stress was 181.2 MPa, as shown in Fig. 5, and so the yield stress ($\sigma_y$) was taken as 181.2 MPa, 362.4 MPa and 543.6 MPa.

In the elastic and inelastic analyses, the tangent rigidities ($(EA)_t$, $(ES_\omega)_t$, $(EI_y)_t$, $(EI_y)_t$, $(EI_\omega)_t$, $(EI_{xy})_t$) were obtained from a nonlinear finite strip analysis[8] of a length of section equal to the local buckle half-wavelength ($l$), In the analyses, the magnitude of the geometric imperfection of the local buckling mode was assumed to be 2 % of the plate thickness. The tangent torsional rigidity $(GJ)_t$ was taken as the full torsional rigidity ($GJ$) in all calculations.

Having determined the resultants ($\lambda\overline{N}$, $\lambda\overline{W}$) and tangent rigidities ($(EA)_t$, $(ES_\omega)_t$, $(EI_y)_t$, $(EI_x)_t$, $(EI_\omega)_t$, $(EI_{xy})_t$, $(GJ)_t$) for increasing levels of axial compression, these values were substituted into eqns (72-75) which were then solved for the length ($L$). The resulting graphs of overall buckling load *vs* length are shown in Figs 6-10, where the overall buckling load ($N_{cr}$) is nondimensionalised with respect to the elastic local buckling load ($N_l$). The columns were assumed to be fixed-ended, and hence the value of $k$=2 was assumed in using eqn. (72).

It appears from Figs 6-10 that the *elastic* overall buckling loads of the locally buckled sections are strongly dependent on the slenderness of the flanges; except for the flexural buckling curve of the 16.3-section which is nearly same as the elastic flexural buckling curve for the undistorted cross-section, see Fig. 6. The latter result is explained with reference to the relatively stocky flanges of the 16.3-section, which ensure similar stress distributions in the flanges of the distorted and undistorted cross-sections at all levels of compression. Since the principal ($x$,$y$)-axes of the 16.3-section are nearly aligned with the flanges and web, as shown in Fig. 5a, the minor axis flexural tangent rigidity $(EI_y)_t=\Delta M_y/-\Delta u''$ is nearly the same as the full flexural rigidity $EI_y$ of the undistorted cross-section. The buckling load is primarily dependent on the term $(EI_y)_t$ and so is nearly the same for the distorted and undistorted 16.3-sections.

The elastic torsional buckling load of the 16.3-section is reduced by local buckling because the sectorial coordinate ($\omega$) is non-zero in the web and hence, the post-local buckling stress redistribution in the web leads to a reduction in the tangent warping rigidity $(EI_\omega)_t=\Delta B/-\Delta\varphi''=\int_A\omega\,\Delta\sigma\,dA/-\Delta\varphi''$, where $\Delta B$ is the change in bimoment.

Local buckling decreases the elastic torsional buckling load for all cross-sections and increasingly so with increasing slenderness of the flanges. For the 65.2-section, the critical mode becomes the torsional mode in the column length range from 3100 mm to 4100 mm, while it is the flexural mode for the undistorted case, as shown in Fig. 10.

In Figs 6-10, the inelastic overall bifurcation curves are terminated at short lengths at the maximum load obtained in the inelastic finite strip local buckling analysis. Thus, the maximum loads shown represent theoretical estimates of the axial section capacity.

The inelastic buckling curves branch off the elastic buckling curves for the distorted cross-sections at the point of first yield. The inelastic buckling load is nearly unchanged after this point when the yield stress ($\sigma_y$) equals the local buckling stress ($\sigma_l$), while, on average, the maximum load at short length is 38% and 82% higher than the elastic local buckling load for $\sigma_y/\sigma_l$ equal to 2 and 3 respectively. The increase depends on the cross-section and is smallest for the 32.6-section for which the local buckling stresses of the flanges and web are equal.

# 5 Conclusions

A theoretical study of locally buckled point symmetric columns compressed between simply supported and fixed ends has been presented, including the derivation of the governing equations for the fundamental and bifurcated states. On the basis of the governing equations, it is shown that the direction of overall flexural buckling changes when the section locally buckles because of coupling between the minor and major flexural displacements. This coupling does not occur according to classical theory where the critical flexural mode is by bending about the minor axis. However, as in classical theory, there is no coupling between the flexural and torsional buckling modes for the locally buckled section.

Equations for the buckling load of point symmetric simply supported and fixed-ended columns are derived and applied to Z-sections. The results show that the torsional buckling load is more reduced by local buckling than the flexural buckling load. This is attributed to the effect of local buckling of the web which leads to greater reductions in the tangent warping rigidity compared to tangent minor axis flexural rigidity. For a Z-section with very slender flanges, this effect can trigger a switch in critical overall buckling mode from the flexural to the torsional mode.

The inelastic analyses showed that yielding does not lead to changes in the critical overall buckling mode for the sections investigated.

# 6 References

[1] Bijlaard, PP and Fisher, GP, Column Strength of H-sections and Square Tubes in Postbuckling Range of Component Plates, *TN 2994*. 1953, NACA: Washington, D.C.

[2] Hancock, GJ, Nonlinear Analysis of Thin Sections in Compression. *Journal of Structural Division, American Society of Civil Engineers*, 1981. **107**(ST3): p. 455-471.

[3] Rasmussen, KJR, Bifurcation of Locally Buckled Members. *Thin-walled Structures*, 1997. **28**(2): p. 117-154.

[4] Young, B and Rasmussen, KJR, Bifurcation of singly symmetric columns. *Thin-walled Structures*, 1997. **Vol. 28**(2): p. 155-177.

[5] Young, B and Rasmussen, KJR, Inelastic Bifurcation of Cold-formed Singly Symmetric Columns. *Thin-walled Structures*, 2000. **36**(3): p. 213-230.

[6] Rasmussen, KJR and Hasham, AS, Flexural and Flexural-Torsional Bifurcation of Locally Buckled Beam-columns. *Thin-walled Structures*, 1998. **29**(1-4): p. 203-233.

[7] Rasmussen, KJR. Torsional Rigidity of Locally Buckled Sections. in *Developments in Mechanics of Structures and Materials, 18th Australasian Conference on the Mechanics of Structures and Materials*. Eds Deeks and Hao, 2004. Perth, Australia: Balkema.

[8] Key, PW and Hancock, GJ, A Finite Strip Method for the Elastic-Plastic Large Displacement Analysis of Thin-Walled and Cold-Formed Steel Sections. *Thin-walled Structures*, 1993. **Vol. 16**: p. 3-29.

[9] Hancock, GJ, Local, Distortional and Lateral Buckling of I-beams. *Journal of the Structural Division, American Society of Civil Engineers*, 1978. **Vol. 104**(ST11): p. 1787-1798.

# Figures

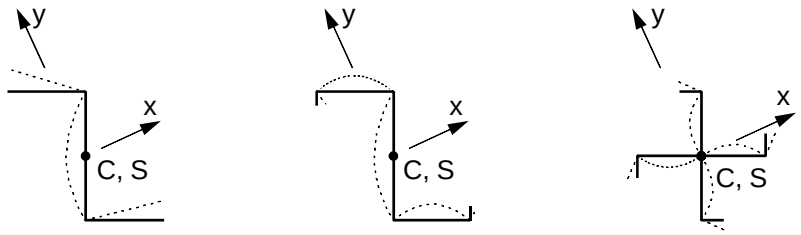


Fig 1: Local buckling of point symmetric sections in compression

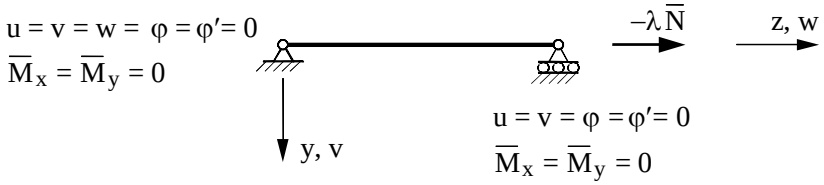


Fig 2: Boundary conditions for simply supported column in compression

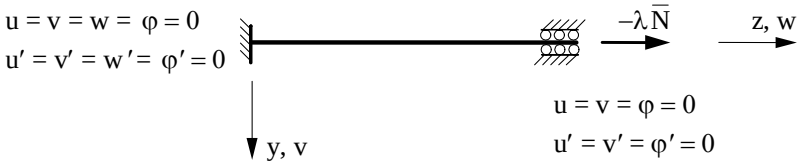


Fig 3: Boundary conditions for fixed-ended column in compression

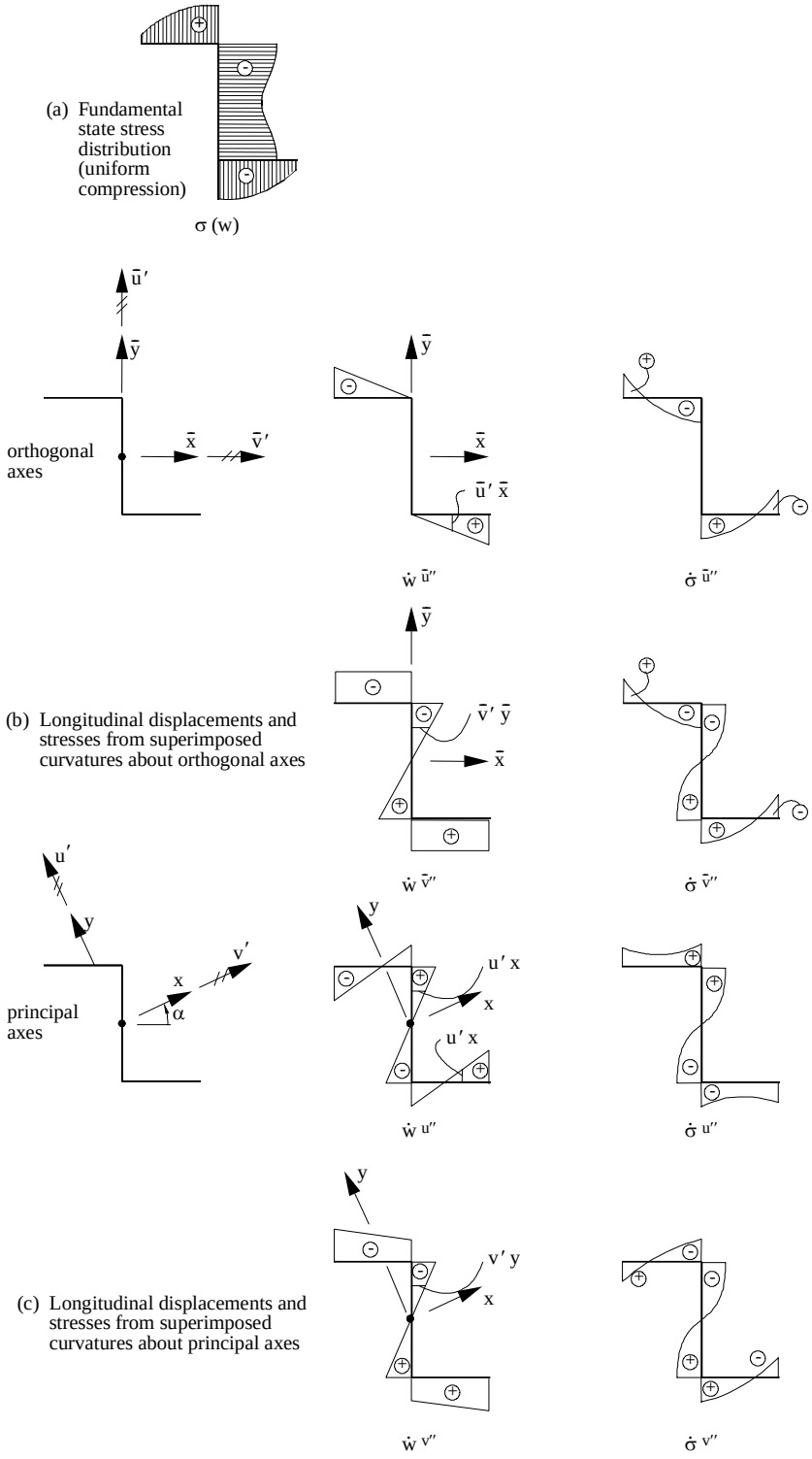


Fig 4: Displacements and stresses arising from rotations about principal and orthogonal axes.

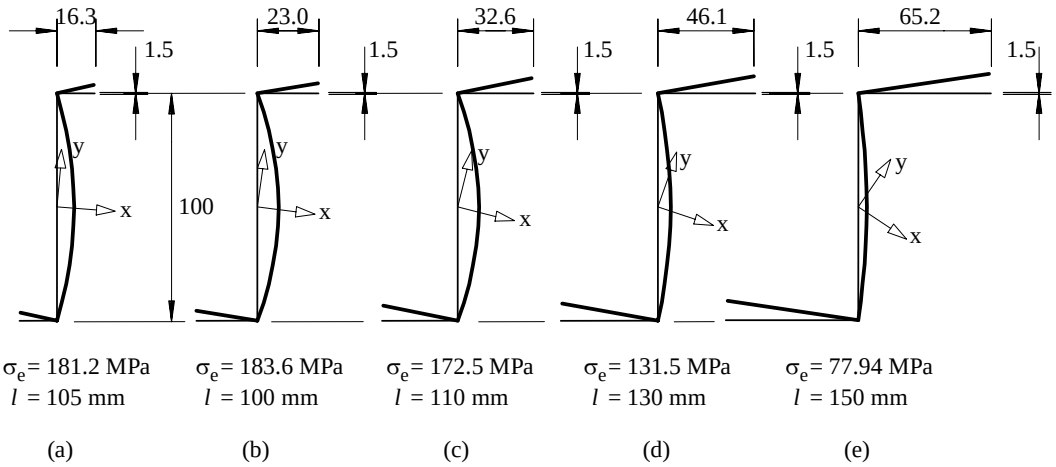


Fig 5: Cross-sections

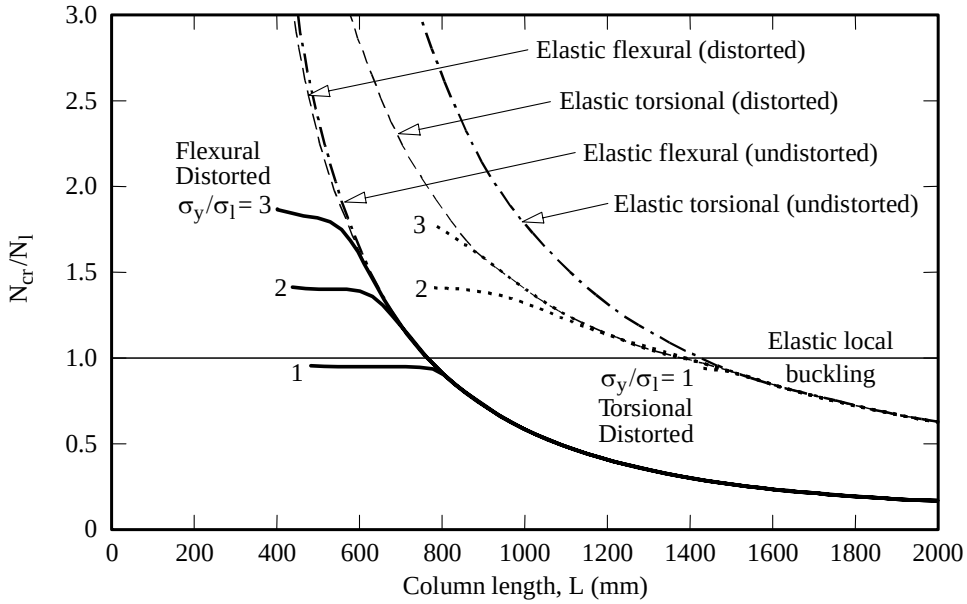


Fig. 6: Buckling curves for 16.3-section

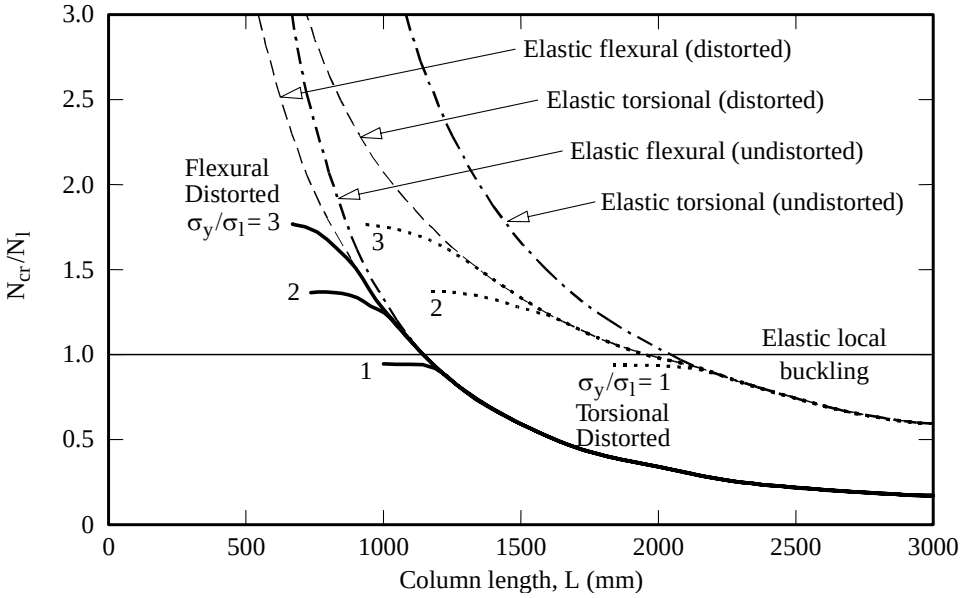


Fig. 7: Buckling curves for 23.0-section

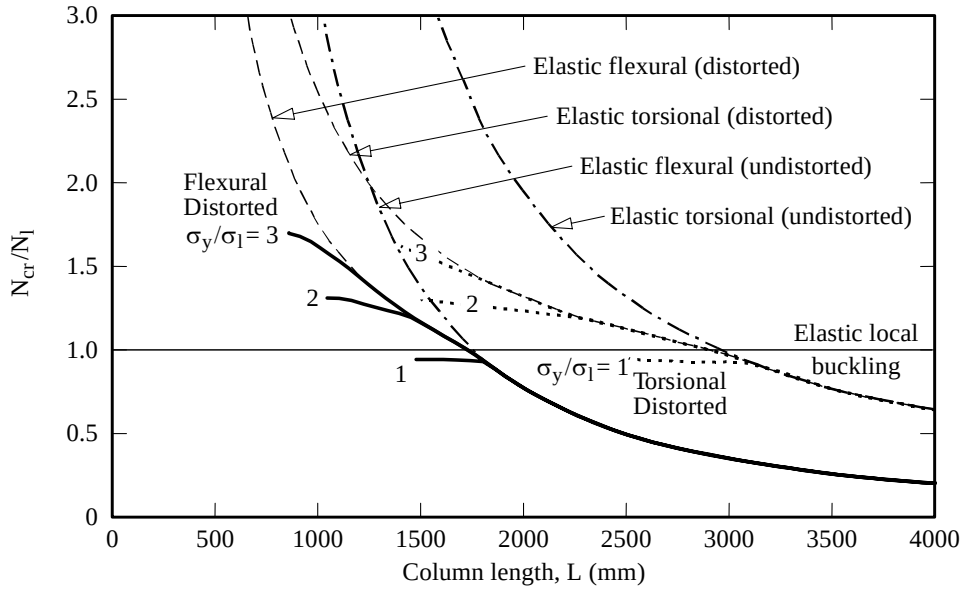


Fig. 8: Buckling curves for 32.6-section

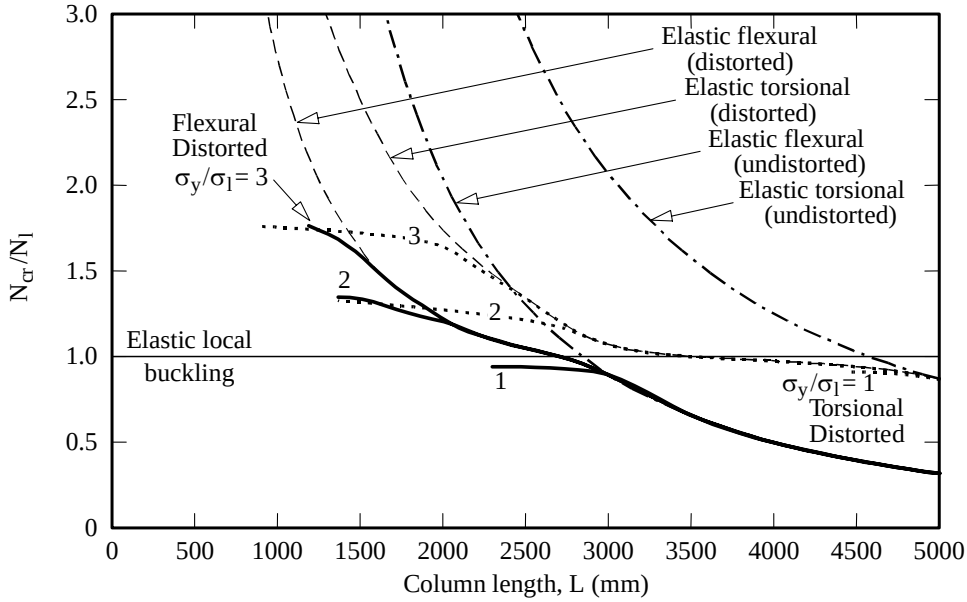


Fig. 9: Buckling curves for 41.6-section

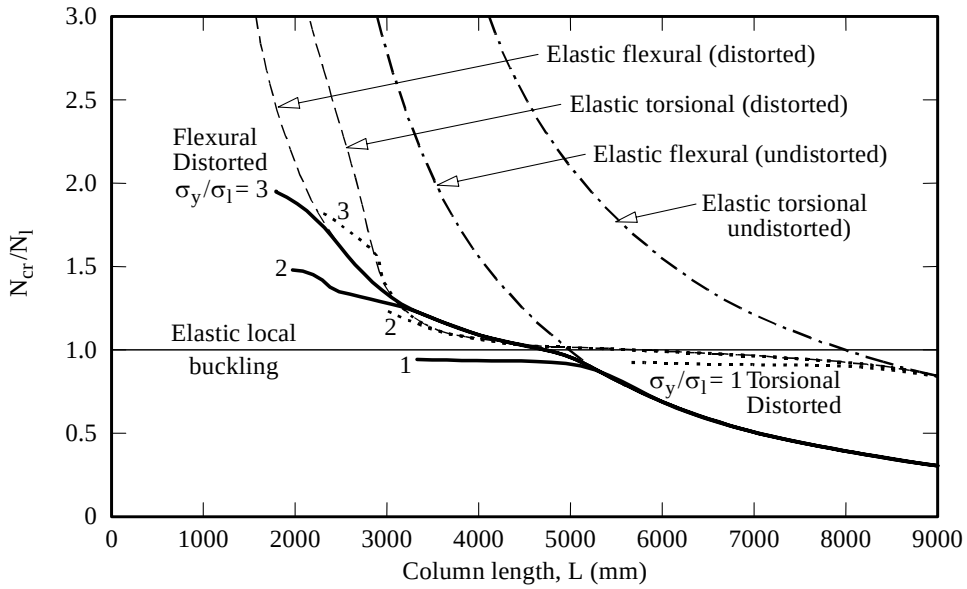


Figure 10. Buckling curves for 65.2-section